frontiers in Chemistry

ORIGINAL RESEARCH
published: 21 March 2022
doi: 10.3389/fchem.2022.841313

Exfoliation of Al-Residual Multilayer MXene Using Tetramethylammonium Bases for Conductive Film Applications

Emi Saita[1†], Masaki Iwata[2†], Yuki Shibata[2†], Yuki Matsunaga[2], Rie Suizu[2,3], Kunio Awaga[2], Jun Hirotani[1,3‡] and Haruka Omachi[2,4*]*

[1]Department of Electronics, Graduate School of Engineering, Nagoya University, Nagoya, Japan, [2]Department of Chemistry, Graduate School of Science, Nagoya University, Nagoya, Japan, [3]PRESTO, Japan Science and Technology Agency, Saitama, Japan, [4]Research Center for Materials Science, Nagoya University, Nagoya, Japan

This study describes the concise exfoliation of multilayer $Ti_3C_2T_x$ MXene containing residual aluminum atoms. Treatment with tetramethylammonium base in a co-solvent of tetrahydrofuran and H_2O produced single-layer $Ti_3C_2T_x$, which was confirmed *via* atomic force microscopy observations, with an electrical conductivity 100+ times that of $Ti_3C_2T_x$ prepared under previously reported conditions. The scanning electron microscopy and X-ray diffraction measurements showed that the exfoliated single-layer $Ti_3C_2T_x$ MXenes were reconstructed to assembled large-domain layered films, enabling excellent macroscale electric conductivity. X-ray photoelectron spectroscopy confirmed the complete removal of residual Al atoms and the replacement of surface fluorine atoms with hydroxy groups. Using the exfoliated dispersion, a flexible transparent conductive film was formed and demonstrated in an electrical application.

Keywords: MXene, exfoliation, tetramethylammonium base, Al etching, transparent conductive film

OPEN ACCESS

Edited by:
Pawel Gluchowski, Włodzimierz Trzebiatowski Institute of Low Temperature and Structure Research (PAS), Poland

Reviewed by:
Asif Shahzad, Kyungpook National University, South Korea
Anna Zielińska-Jurek, Gdansk University of Technology, Poland

***Correspondence:**
Jun Hirotani
hirotani.jun.7v@kyoto-u.ac.jp
Haruka Omachi
omachi@chem.nagoya-u.ac.jp

‡Present address: Jun Hirotani, Department of Micro Engineering, Graduate School of Engineering, Kyoto University, Kyoto, Japan

†These authors have contributed equally to this work and share first authorship

Specialty section:
This article was submitted to Nanoscience, a section of the journal Frontiers in Chemistry

Received: *22 December 2021*
Accepted: *23 February 2022*
Published: *21 March 2022*

Citation:
Saita E, Iwata M, Shibata Y, Matsunaga Y, Suizu R, Awaga K, Hirotani J and Omachi H (2022) Exfoliation of Al-Residual Multilayer MXene Using Tetramethylammonium Bases for Conductive Film Applications. Front. Chem. 10:841313. doi: 10.3389/fchem.2022.841313

INTRODUCTION

Since first reported by Naguib et al. (2011), MXenes have attracted wide attention as novel analogs of two-dimensional layer nanomaterials such as graphene, hexagonal boron nitride, and transition-metal dichalcogenides. MXenes show high mechanical durability and transparency conferred by the layer structure, along with unique chemical natures and excellent electrical characteristics (Naguib et al., 2014; Verger et al., 2019; Wang et al., 2020). The general formula of MXenes is $M_{n+1}X_nT_x$ (M: early transition metals, X: carbon and/or nitrogen, T: a terminal functional group such as F, OH, O). The electronic band structures of MXenes depends on the combination of their M, X, and T atoms. For instance, the simple titanium carbide family (e.g., Ti_2CT_x, $Ti_3C_2T_x$) shows a metallic property with high charge-carrier density, whereas $Cr_2TiC_2F_2$ and $Cr_2TiC_2(OH)_2$ are thought to behave as semiconductors. Moreover, MXenes with hydrophilic terminal functional groups are dispersible in water and polar organic solvents without surfactants; accordingly unlike other nanomaterials, they can act as scaffolds for chemical modification. These advantages are expected to be exploited in a wide range of applications, such as Li- or Na-ion batteries (Naguib et al., 2012; Liang et al., 2015; Natu et al., 2018), transparent conductive films (Dillon et al., 2016; Hantanasirisakul et al., 2016; Zhou et al., 2021), catalysts for hydrogen evolution (Seh et al., 2016; Intikhab et al., 2019) and supercapacitors (Lukatskaya et al., 2013; Dall'Agnese et al., 2015; Wang et al., 2015).

Typically, MXenes are produced from the MAX phase ($M_{n+1}AlX_n$) in a hydrogen fluoride (HF) treatment, which removes the atomically thin layer of aluminum atoms (Naguib et al., 2011; Lukatskaya et al., 2013; Luo et al., 2016). To date, researchers can easily access commercially available MXenes, without using a hazardous HF acid (the highest hazard level in the health section of NFPA 704). However, these MXenes maintain their multilayer structure *via* covalent bonding between the layers and residual Al atoms. Such MXenes are rarely dispersed and immediately precipitate out even after vigorous sonication. Furthermore, films prepared from filtrates of these MXenes are electrically non-conductive. To realize the above applications, conductive liquid-state MXene materials are desired for fabrication processes such as spray coating, spin cast, and filtration. Therefore, a concise and HF-free method that exfoliates and disperses MXene as a single-layer nanomaterial by removing the Al atoms is required.

This work reports on the exfoliation of Al-residual multilayer $Ti_3C_2T_x$, the most commonly used conductive MXene, with organic bases containing a tetramethylammonium cation. This treatment effectively removes the interlayer Al atoms from the MXenes. The $Ti_3C_2T_x$ exfoliated in a co-solvent of tetrahydrofuran (THF) and H_2O exhibited superior electrical conductivity. We also demonstrate the application of flexible transparent conductive films fabricated by spray-gun coating with the exfoliated $Ti_3C_2T_x$ dispersion.

EXPERIMENTAL SECTION

Sample Preparation

$Ti_3C_2T_x$ MXene (Japan Material Technologies Corporation, 4 mg), 0.2 mmol of tetramethylammonium reagent (**Table 1**), and 2 ml of solvent were added to a vial containing a magnetic stirring bar. After stirring at room temperature for 24 h, the mixture was transferred to a 15-ml conical tube with deionized (DI) water (0.2 ml × 4), which were degassed by N_2 bubbling for 30 min prior to use. After adding 2-propanol (2 ml), the mixture was centrifuged at 4,500 rpm for 5 min and the supernatant was removed. After adding 2 ml of DI water to the sediment, the mixture was dispersed in a bath-sonicator (BM EQUIPMENT, Nanoruptor NR-350) for 40 min and centrifuged at 433 *g* for 30 min. The resulting supernatant was collected as the MXene dispersion. The exfoliation yield was estimated from the intensity of the absorption spectrum at 800 nm, recorded on an ultraviolet–visible spectrophotometer (JASCO V-770) after freeze-drying treatment with EYELA FDS-1000.

The sheet resistances (R_s, Ω/sq) of the films were measured using the four-probe method with a Loresta-AX resistivity meter (MCP-TP06P, Mitsubishi Chemical Analytech). Thick MXene films were prepared by vacuum filtration of the dispersions (0.1 mg in 50 ml DI water) on a MF-Millipore 47-mm MCE membrane filter (0.05-μm pore size).

Characterization

The optical absorption spectra of the dispersion sample were recorded on an ultraviolet–visible spectrophotometer (V-770, JASCO). Raman spectra in the radial-breathing mode region were recorded on an inVia Raman Microscope (Renishaw) excited by 785-nm laser light. A single-monochromator micro-Raman spectrometer was employed in the back-scattering configuration. The sample dispersions were drop-casted onto a silicon wafer before the measurement. X-ray photoelectron spectroscopy (XPS) data were obtained using an ESCALAB XI + spectrometer (Thermo Fisher Scientific) using 300 W Al–Ka radiation. To exclude the substrate signals, a highly concentrated MXene dispersion was drop-coated several times onto a Si/SiO_2 wafer to form a thick MXene film (>10 nm). Atomic force microscopy (AFM) measurements were acquired using a Dimension Fastscan AFM with a NanoScope V stage controller (Bruker). The samples for AFM observation were prepared by spin-coating the Si/SiO_2 wafer with 10 μl of the MXene dispersion at 400 rpm for 60 s, followed by 1,000 rpm for 60 s and 1,600 rpm for 60 s. Scanning electron microscopy (SEM) measurements were conducted in an S-4300 (Hitachi) or an ETHOS NX5000 (Hitachi). X-ray diffraction (XRD) spectra were obtained by a SmartLab (Rigaku) through Cu Kα radiation.

Fabrication of Flexible Transparent Conductive Films

Polyethylenenaphthalete (PEN) films with a thickness of 100 μm and DuPont Films (Q65FA) were surface-treated with a plasma cleaner (YAMATO PR500) at 100 W for 10 min. The MXene dispersion diluted with methanol was coated using a spray-gun (ANEST IWATA HP-TR1). The spray-coated films were dried at 30°C for 16 h under vacuum conditions (<5 Pa). The transparency was determined by the absorption spectra recorded on an ultraviolet–visible spectrophotometer (V-770, JASCO). The sheet resistance (R_s, Ω/sq) of the films was measured using the four-probe method with a Loresta-AX resistivity meter (MCP-TP06P, Mitsubishi Chemical Analytech).

RESULTS AND DISCUSSION

Optimization of Exfoliation Conditions

Initially, etching reagents other than HF acid were explored for removing residual Al atoms from $Ti_3C_2T_x$ MXene. Prior to the investigation, we tested dimethyl sulfoxide (DMSO) (Mashtalir et al., 2013) and tetrabutylammonium cations (Naguib et al., 2015) as intercalation agents that can expand the inter layer distance of MXenes. These agents did not exfoliate the Al-residual multilayered $Ti_3C_2T_x$ MXene. After screening a variety of organic and inorganic fluoride reagents, it was found that only tetramethylammonium fluoride (Me_4NF) in DMSO solvent obtained the desired MXene dispersion in 22% yield (**Figure 1A**). The optical absorption spectrum of the dispersion exhibited a peak around 800 nm, consistent with reported examples (Li et al., 2017) (**Figure 1B**). Because tetramethylammonium hydroxide (Me_4NOH) can etch the MAX phase (Xuan et al., 2016; Yang et al., 2018), we supposed that the tetramethylammonium cations were suitably sized to penetrate the inter layers of MXenes, which were geometrically restricted by bonding with aluminum atoms.

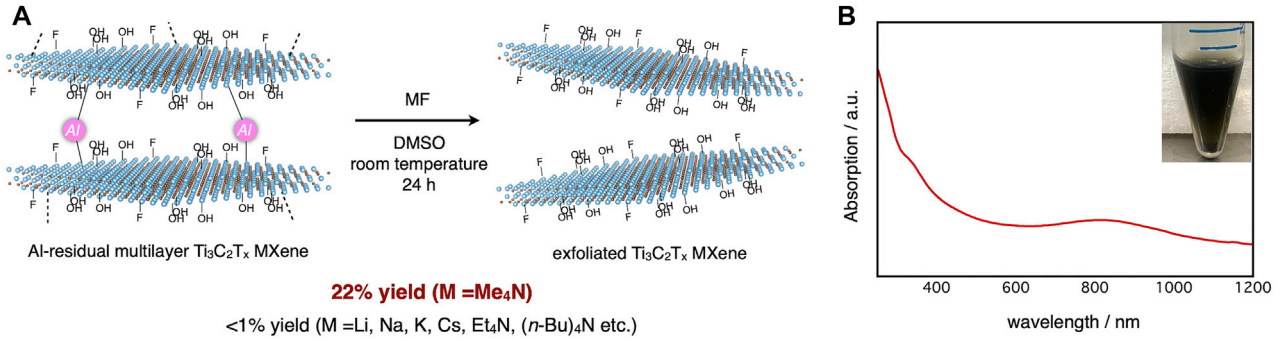

FIGURE 1 | (A) Exfoliation of Al-residual $Ti_3C_2T_x$ MXene with Me_4NF; **(B)** Optical absorption spectrum (main) and typical photograph (inset) of $Ti_3C_2T_x$ MXene dispersion.

TABLE 1 | Optimized reaction conditions for exfoliating multilayer $Ti_3C_2T_x$ MXene.

Entry	Reagent	Solvent	Time [h]	Yield [%]	*Rs* (SD) [Ω/sq.]
1	$Me_4NF{\cdot}4H_2O$	DMSO	24	22	1.4×10^4 (2.1×10^3)
2	Me_4NOAc	DMSO	24	4	3.8×10^4 (5.9×10^3)
3	$Me_4NOH{\cdot}5H_2O$	DMSO	24	12	7.1×10^3 (9.1×10^2)
4	Me_4NCl	DMSO	24	<1	—
5	Me_4NBr	DMSO	24	<1	—
6	Me_4NBF_4	DMSO	24	<1	—
7	$Me_4NOH{\cdot}5H_2O$	H_2O	24	43	2.0×10^4 (9.1×10^2)
8	$Me_4NOH{\cdot}5H_2O$	THF	24	15	2.0×10^3 (2.5×10^2)
9	$Me_4NOH{\cdot}5H_2O$	CH_3CN	24	<1	—
10	$Me_4NOH{\cdot}5H_2O$	NMP	24	<1	—
11	$Me_4NOH{\cdot}5H_2O$	CH_3OH	24	<1	—
12	$Me_4NOH{\cdot}5H_2O$	THF/H_2O[a]	24	46	2.0×10^3 (2.5×10^2)
13	$Me_4NOH{\cdot}5H_2O$	THF/H_2O[a]	72	59	1.4×10^3 (93)
14[b]	$Me_4NOH{\cdot}5H_2O$	THF/H_2O[a]	72	5	2.7×10^2 (6.2)
15[b]	$Me_4NOH{\cdot}5H_2O$	THF/H_2O[a]	120	20	1.5×10^2 (8.8)

[a]*Solvent ratio (v/v): THF/H_2O = 10/1.*
[b]*Without sonication treatment.*

Next, we investigated the effect of the counter anions on tetramethylammonium salts (**Table 1**). Adding Me_4NOH and tetramethylammonium acetate (Me_4NOAc) to Me_4NF enabled the exfoliation of $Ti_3C_2T_x$ MXene, implying that basic counter anions are required for removing the aluminum atoms (entries 1–6). The sheet resistance of the film fabricated with the Me_4NOH dispersion was 7.1×10^3 Ω/sq., lower than those of the films produced from Me_4NF-exfoliated and Me_4NOAc-exfoliated MXenes (1.4×10^4 and 3.8×10^4 Ω/sq., respectively). At this stage, we selected Me_4NOH as the etching reagent and screened several solvents to improve the exfoliation efficiency and electrical conductivity. When the reaction was performed in aqueous solution under conditions similar to the reported etching conditions of MAX phases, the exfoliation reached 43% yield, but the film conductivity reduced to an undesirable 2.0×10^4 Ω/sq. (entry 7 of **Table 1**). The exfoliation yield was only 15% in tetrahydrofuran (THF) solvent and was less than 1% in the other organic solvents (entries 8–11 in **Table 1**). The sheet resistance of the exfoliated MXene (2.0×10^3 Ω/sq.) was three times lower in THF than in DMSO. Surprisingly, a mixed solvent of THF and H_2O was effective for both exfoliation (46% yield) and conductivity (2.0×10^3 Ω/sq.). Extending the reaction time also enhanced the exfoliation yield (entries 12 and 13 in **Table 1**). Under these conditions, MXenes were spontaneously exfoliated without the sonication treatment, and the sheer resistance was drastically decreased to ca. 2.0×10^2 Ω/sq. (entries 14 and 15 in **Table 1**). Eventually, we found that reacting MXene with Me_4NOH in THF/H_2O solvent for 120 h produced the desired MXene dispersion, balancing the exfoliation efficiency with high conductivity (entry 15 in **Table 1**).

Microscopic Observations and Assembled Structural Analysis

Next, the exfoliated $Ti_3C_2T_x$ MXenes prepared by the spin-coating method were characterized by AFM. A typical AFM image is shown in **Figure 2A** and the height profile is shown in **Figure 2B**. The MXene flakes were approximately 2 nm thick, consistent with previous measurements of single-layer MXene (Xuan et al., 2016). Without the sonication treatment, the exfoliated sample presented MXene sheets with an approximate size of >5 μm (**Figure 2A**), but after sonication, small flakes (<500 nm in size) were observed

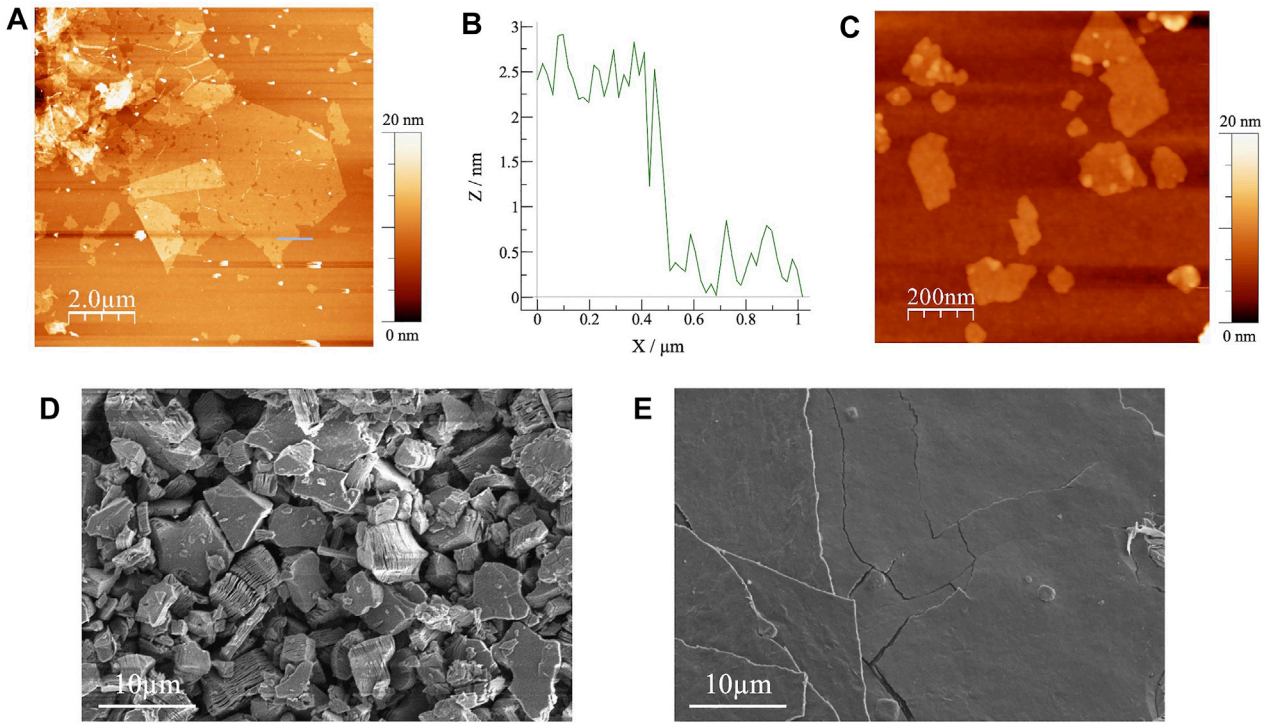

FIGURE 2 | (A) AFM image and **(B)** the corresponding height profile of exfoliated $Ti_3C_2T_x$ MXene without sonication; **(C)** AFM image of exfoliated $Ti_3C_2T_x$ MXene prepared by the sonication treatment; SEM images of **(D)** pristine and **(E)** exfoliated $Ti_3C_2T_x$ MXene.

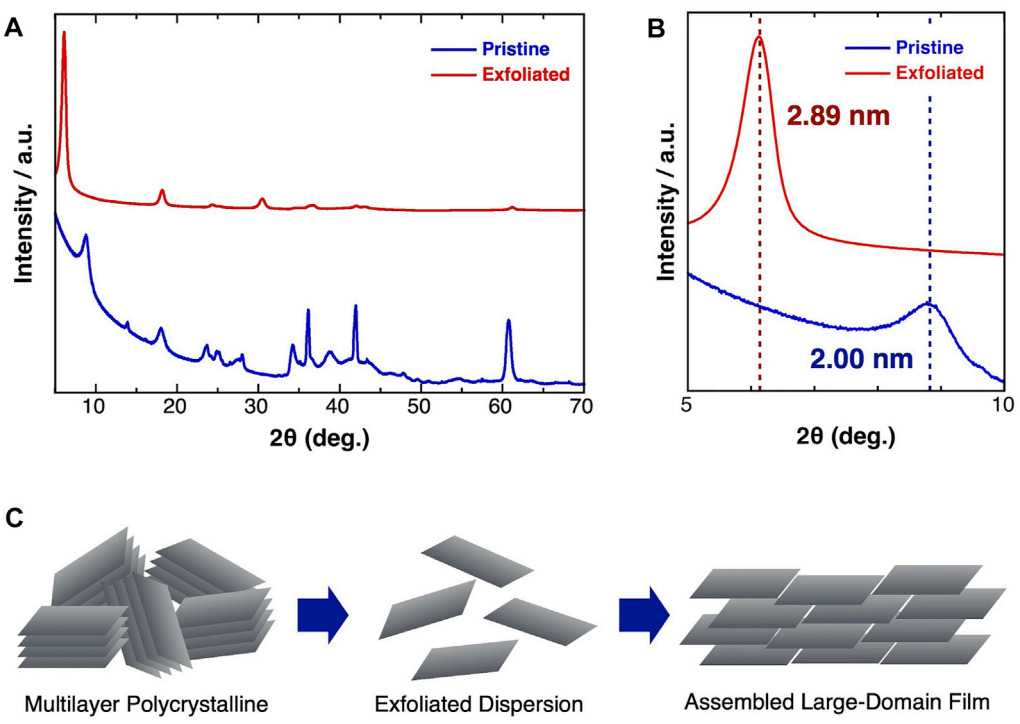

FIGURE 3 | (A) Whole region and **(B)** magnified XRD pattern of (blue) pristine and (red) exfoliated $Ti_3C_2T_x$ MXene. **(C)** Schematic image of the exfoliation process and the film formation process of the exfoliated MXene.

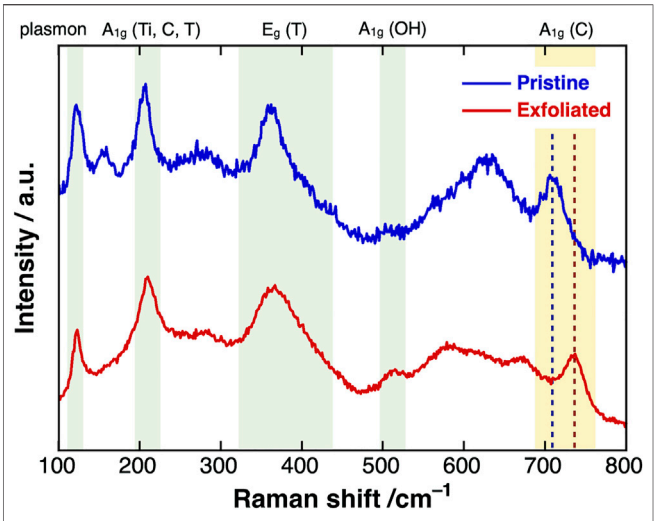

FIGURE 4 | Raman spectra of (blue) pristine and (red) exfoliated $Ti_3C_2T_x$ MXene.

(**Figure 2C**). Because tiny defective pinholes were detected on the surface of the large MXene sheet (**Figure 2A**), it appeared that sonication proceeded by tearing the sheets into small pieces. In the macroscale film, the sheet resistance would be increased by the increased number of contact-resistance points between the networked MXene flakes.

Figure 2D shows a SEM image of pristine $Ti_3C_2T_x$ MXene filtrated on the MCE membrane filter. Although the inter layer distances were slightly expanded, most of the flakes maintained the multilayer structure after the sonication treatment. Judging from the polycrystalline-like morphology, a conductivity network is not easily formed in this film. The lateral size of the multilayer $Ti_3C_2T_x$ was 5–10 μm, compatible to that of exfoliated $Ti_3C_2T_x$ in the AFM measurement. Conversely, an SEM image of the exfoliated $Ti_3C_2T_x$ confirmed the formation of paper-like film structures (**Figure 2E**). In addition, larger domain films, compared with the observed lateral size in AFM, were obtained by the random stacking of the exfoliated flakes, which were similar to other two-dimensional nanomaterials (Dikin et al., 2007; Yun et al., 2017).

The detailed structural changes during the exfoliation and film formation processes were uncovered using XRD measurements (**Figure 3**). The XRD pattern of the pristine $Ti_3C_2T_x$ was in good agreement with that of the HF-treated $Ti_3C_2T_x$ (Naguib et al., 2011) (**Figure 3A**). After the exfoliation process, the (002) peak ($2\theta = 8.84^\circ$) shifted to a lower angle ($2\theta = 6.12^\circ$), corresponding to an expansion of the average inter layer spacing from 2.00 to 2.88 nm (**Figure 3B**). A similar expansion of the inter layer distance was reported in previous exfoliation studies using organic intercalation agents (Mashtalir et al., 2013; Naguib et al., 2015). Moreover, the relative intensity of the (002) peak in the spectrum of the exfoliated $Ti_3C_2T_x$ was obviously

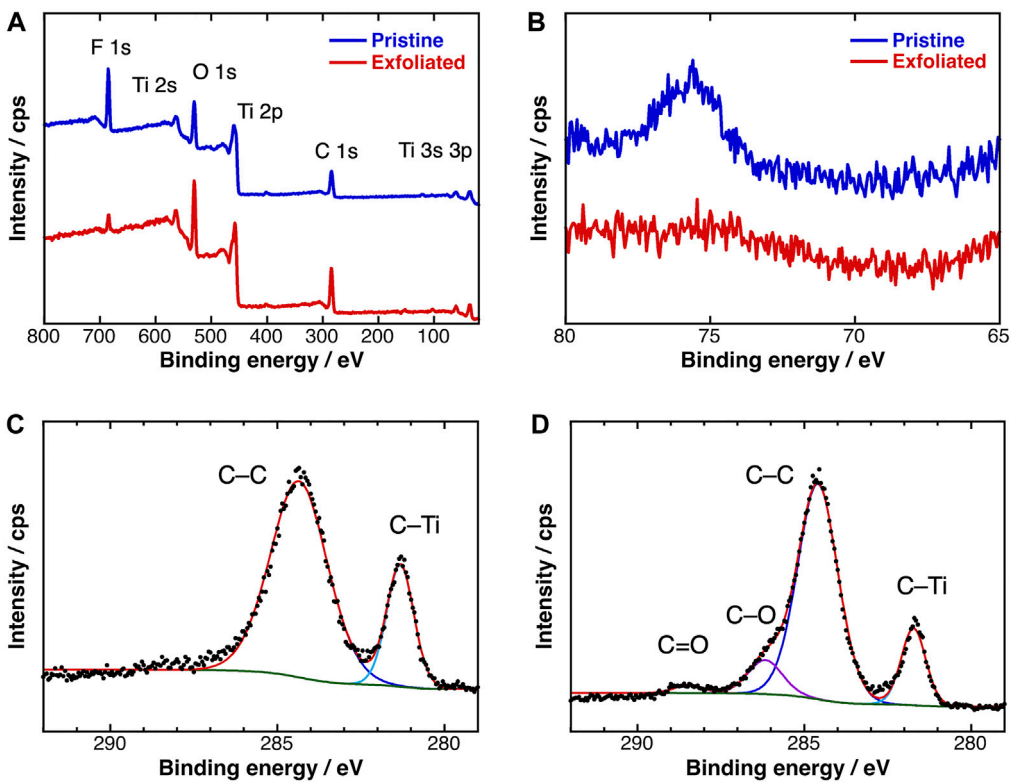

FIGURE 5 | (A) Survey and **(B)** Al 2p XPS spectra of (blue) pristine and (red) exfoliated $Ti_3C_2T_x$ MXene; C 1p XPS spectra of **(C)** pristine and **(D)** exfoliated $Ti_3C_2T_x$ MXene.

TABLE 2 | XPS atomic percentages of pristine and exfoliated $Ti_3C_2T_x$ MXene.

Sample	Atomic content [%]				
	F 1s	O 1s	Ti 2p	C 1s	Al 2s
Pristine	21.5	22.9	18.8	35.2	1.6
Exfoliated	5.4	31.0	17.7	45.9	<0.1

enhanced, indicating that the single-layer flakes were stacked with a well-alignment. **Figure 3C** shows a schematic image of the exfoliation and film formation processes. The multilayer Al-residual $Ti_3C_2T_x$ was exfoliated by the treatment with Me_4NOH. Thereafter, the obtained single-layer $Ti_3C_2T_x$ dispersion was reconstructed to assembled large-domain layered films, enabling excellent macroscale electric conductivity.

Chemical Structure Characterizations

We now report the Raman spectra of pristine and exfoliated MXenes excited by a 785-nm laser (**Figure 4**). The sharp peaks at 106, 204, and 380 cm^{-1} in both spectra were assigned to the plasmonic, A_{1g} (Ti, C, T), and E_g (T) peaks of $Ti_3C_2T_x$ MXenes, respectively. After exfoliation, the A1g peak originating from carbon atoms shifted from 709 to 737 cm^{-1}, close to the typical value of single-layer $Ti_3C_2T_x$ MXene. This phenomenon strongly suggested that most of the exfoliated MXenes in the dispersion maintained the single-layer state (Sarycheva and Gogotsi, 2020). In addition, the intensity of the A_{1g} peak of the hydroxy groups at around 510 cm^{-1} and the full width at half maximum of the E_g (T) peak were slightly increased, implying that surface oxidation occurred during the etching reaction.

The chemical structures of the MXenes were further clarified in XPS measurements. The survey spectra of pristine and exfoliated MXenes presented the distinct peaks of titanium (3p: 36 eV, 3s: 61 eV, 2p: 459 eV, and 2s: 563 eV), carbon (1s: 284 eV), oxygen (1s: 531 eV), and fluorine (1s: 691 eV) atoms (**Figure 5A**). The peak assigned to Al 2p was clearly absent in the high-resolution spectrum of the exfoliated sample (**Figure 5B**). As expected, the content percentage of aluminum atoms dropped from 1.6 to <0.1 at.% (**Table 2**). The F 1s peak was also depressed in the survey spectrum of the exfoliated sample. The intensity of the F 1s peaks drastically reduced from 21.5 to 5.4, indicating that the substitution reaction of Ti–F to Ti–OH bonds was promoted by the Me_4NOH reagent. Meanwhile, the hydroxy group population increased, consistent with the behavior of the A_{1g} (OH) peak in the Raman spectrum.

Figures 5C,D display the HR C 1s spectra of the pristine and exfoliated MXenes, respectively. After separating the peaks, the major peaks at 281 and 284 eV were assigned to C–Ti and C–C bonds, respectively. In the spectrum of the exfoliated sample, the shoulder band at 286.2 eV originated from the carbon–oxygen single bond (C–O) of hydroxy groups, and the negligibly weak peak at 288.5 eV was attributable to carbon–oxygen double bonds (C=O). The generation of these oxidized carbon peaks suggest that partial chemical etching of the titanium atoms with Me_4NOH exposed the inner carbon atoms. Such structural defects are consistent with the pinholes observed in the AFM image of the large-sized MXene sheets.

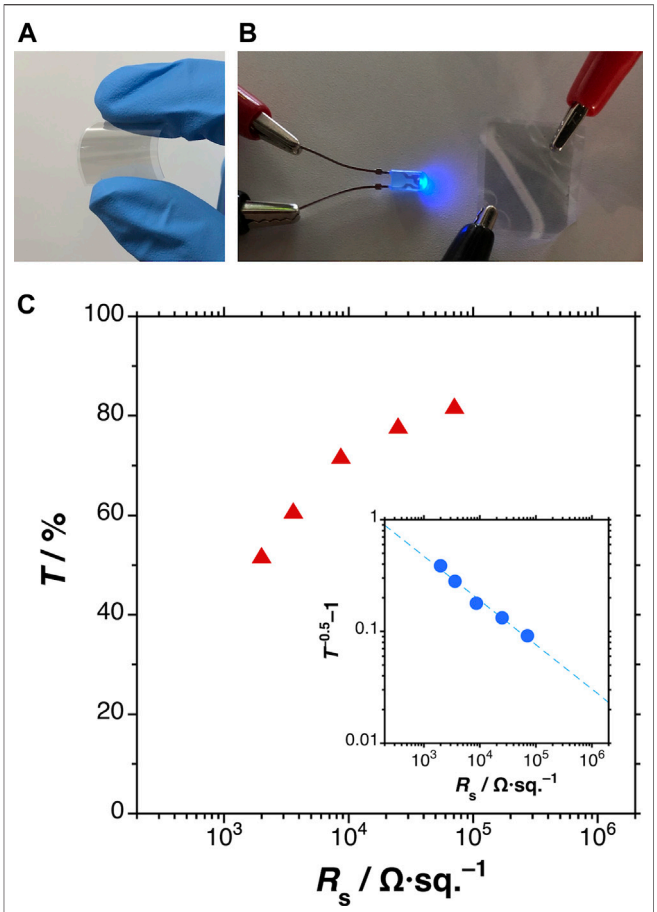

FIGURE 6 | (A,B) Typical photographs of the fabricated MXene transparent conductive films; **(C)** plots of transmittance at 600 nm (main) and $T^{-0.5}$–1 (inset) versus average sheet resistance of the MXene films.

Application to Flexible Transparent Conductive Films

Finally, the transparent conductive MXene films were demonstrated in an application (**Figure 6**). The MXene films were formed on a PEN film by spraying of the dispersion diluted in methanol solvent. **Figures 6A,B** are typical photographs of the fabricated MXene films. The film was bendable (**Figure 5A**) and sufficiently electrically conductive (**Figure 6B**). **Figure 6C** plots the transmittance at a wavelength of 600 nm versus the average sheet resistance of various MXene films. The R_s at 78% transmittance was 2.5×10^4 Ω/sq., comparable to those of previous spray-coated examples (Hantanasirisakul et al., 2016; Zhou et al., 2021). The inset of **Figure 6C** plots $T^{-0.5}$–1 as a function of R_s. The resulting bulk-type conductivity curve is consistent with those of other MXene films (Dillon et al., 2016).

CONCLUSION

In conclusion, we exfoliated Al-residual multilayered $Ti_3C_2T_x$ MXene with Me_4NOH in THF/H_2O co-solvent. $Ti_3C_2T_x$, exfoliated into single layers without sonication, as confirmed in

AFM observations and Raman spectroscopy. The conductivity was 100+ times higher than in films exfoliated under previously reported aqueous conditions. Moreover, transparent conductive films were formed on flexible PEN substrates using the synthesized $Ti_3C_2T_x$ dispersion. XPS measurements of the exfoliated samples clarified that the Al atoms were removed and the Ti–F bonds transformed into Ti–OH bonds. The generated hydroxy groups, which can convert to a variety of functional groups, expand the feasibility of MXene as a conductive support material in catalysis, battery, and electrochemical applications. Thiol (Omachi et al., 2020) or amino groups (Matsumoto et al., 2020) can immobilize the metal clusters and nanomaterials, realizing novel conductive nanohybrid materials rather than the existing graphite or graphene examples. Further chemical modification of $Ti_3C_2T_x$ toward electrode applications in battery systems is ongoing in our laboratory.

DATA AVAILABILITY STATEMENT

The original contributions presented in the study are included in the article/Supplementary Material, further inquiries can be directed to the corresponding authors.

AUTHOR CONTRIBUTIONS

HO and JH conceived the study. ES, MI, YS, JH, and HO developed the exfoliation conditions and performed the characterizations. RS and KA conducted the XRD measurement. YS and YM performed the conductive film applications. HO mainly prepared the manuscript and all authors discussed results, helped edit the manuscript and gave final approval for publication.

FUNDING

This work received financial support from JST CREST (19203618) and PRESTO (JPMJPR20B6), and JSPS Grant-in-Aid for Scientific Research (JP19H02168, 20KK0087).

ACKNOWLEDGMENTS

We thank Satomi Ogasawara (Nagoya Univ.) for supporting the experiments and Ayako Suzuki (Nagoya Univ.) for helping with the XPS measurements. We also acknowledge Prof. Kenichiro Itami for the use of the AFM and Raman equipment.

REFERENCES

Dall'Agnese, Y., Taberna, P.-L., Gogotsi, Y., and Simon, P. (2015). Two-dimensional Vanadium Carbide (MXene) as Positive Electrode for Sodium-Ion Capacitors. *J. Phys. Chem. Lett.* 6, 2305–2309. doi:10.1021/acs.jpclett.5b00868

Dikin, D. A., Stankovich, S., Zimney, E. J., Piner, R. D., Dommett, G. H. B., Evmenenko, G., et al. (2007). Preparation and Characterization of Graphene Oxide Paper. *Nature* 448, 457–460. doi:10.1038/nature06016

Dillon, A. D., Ghidiu, M. J., Krick, A. L., Griggs, J., May, S. J., Gogotsi, Y., et al. (2016). Highly Conductive Optical Quality Solution-Processed Films of 2D Titanium Carbide. *Adv. Funct. Mater.* 26, 4162–4168. doi:10.1002/adfm.201600357

Hantanasirisakul, K., Zhao, M. Q., Urbankowski, P., Halim, J., Anasori, B., Kota, S., et al. (2016). Fabrication of Ti 3 C 2 T X MXene Transparent Thin Films with Tunable Optoelectronic Properties. *Adv. Electron. Mater.* 2, 1600050. doi:10.1002/aelm.201600050

Intikhab, S., Natu, V., Li, J., Li, Y., Tao, Q., Rosen, J., et al. (2019). Stoichiometry and Surface Structure Dependence of Hydrogen Evolution Reaction Activity and Stability of MoxC MXenes. *J. Catal.* 371, 325–332. doi:10.1016/j.jcat.2019.01.037

Li, R., Zhang, L., Shi, L., and Wang, P. (2017). MXene Ti3C2: An Effective 2D Light-To-Heat Conversion Material. *ACS Nano* 11, 3752–3759. doi:10.1021/acsnano.6b08415

Liang, X., Garsuch, A., and Nazar, L. F. (2015). Sulfur Cathodes Based on Conductive MXene Nanosheets for High-Performance Lithium-Sulfur Batteries. *Angew. Chem. Int. Ed.* 54, 3907–3911. doi:10.1002/anie.201410174

Lukatskaya, M. R., Mashtalir, O., Ren, C. E., Dall'Agnese, Y., Rozier, P., Taberna, P. L., et al. (2013). Cation Intercalation and High Volumetric Capacitance of Two-Dimensional Titanium Carbide. *Science* 341, 1502–1505. doi:10.1126/science.1241488

Luo, J., Tao, X., Zhang, J., Xia, Y., Huang, H., Zhang, L., et al. (2016). Sn4+ Ion Decorated Highly Conductive Ti3C2 MXene: Promising Lithium-Ion Anodes with Enhanced Volumetric Capacity and Cyclic Performance. *ACS Nano* 10, 2491–2499. doi:10.1021/acsnano.5b07333

Mashtalir, O., Naguib, M., Mochalin, V. N., Dall'Agnese, Y., Heon, M., Barsoum, M. W., et al. (2013). Intercalation and Delamination of Layered Carbides and Carbonitrides. *Nat. Commun.* 4, 1716. doi:10.1038/ncomms2664

Matsumoto, K., Ueno, K., Hirotani, J., Ohno, Y., and Omachi, H. (2020). Fabrication of Carbon Nanotube Thin Films for Flexible Transistors by Using a Cross-Linked Amine Polymer. *Chem. Eur. J.* 26, 6118–6121. doi:10.1002/chem.202000228

Naguib, M., Come, J., Dyatkin, B., Presser, V., Taberna, P.-L., Simon, P., et al. (2012). MXene: a Promising Transition Metal Carbide Anode for Lithium-Ion Batteries. *Electrochemistry Commun.* 16, 61–64. doi:10.1016/j.elecom.2012.01.002

Naguib, M., Kurtoglu, M., Presser, V., Lu, J., Niu, J., Heon, M., et al. (2011). Two-Dimensional Nanocrystals Produced by Exfoliation of Ti3AlC2. *Adv. Mater.* 23, 4248–4253. doi:10.1002/adma.201102306

Naguib, M., Mochalin, V. N., Barsoum, M. W., and Gogotsi, Y. (2014). 25th Anniversary Article: MXenes: a New Family of Two-Dimensional Materials. *Adv. Mater.* 26, 992–1005. doi:10.1002/adma.201304138

Naguib, M., Unocic, R. R., Armstrong, B. L., and Nanda, J. (2015). Large-scale Delamination of Multi-Layers Transition Metal Carbides and Carbonitrides "MXenes". *Dalton Trans.* 44, 9353–9358. doi:10.1039/c5dt01247c

Natu, V., Clites, M., Pomerantseva, E., and Barsoum, M. W. (2018). Mesoporous MXene Powders Synthesized by Acid Induced Crumpling and Their Use as Na-Ion Battery Anodes. *Mater. Res. Lett.* 6, 230–235. doi:10.1080/21663831.2018.1434249

Omachi, H., Inoue, T., Hatao, S., Shinohara, H., Criado, A., Yoshikawa, H., et al. (2020). Concise, Single-Step Synthesis of Sulfur-Enriched Graphene: Immobilization of Molecular Clusters and Battery Applications. *Angew. Chem. Int. Ed.* 59, 7836–7841. doi:10.1002/anie.201913578

Sarycheva, A., and Gogotsi, Y. (2020). Raman Spectroscopy Analysis of the Structure and Surface Chemistry of Ti3C2Tx MXene. *Chem. Mater.* 32, 3480–3488. doi:10.1021/acs.chemmater.0c00359

Seh, Z. W., Fredrickson, K. D., Anasori, B., Kibsgaard, J., Strickler, A. L., Lukatskaya, M. R., et al. (2016). Two-dimensional Molybdenum Carbide (MXene) as an Efficient Electrocatalyst for Hydrogen Evolution. *ACS Energ. Lett.* 1, 589–594. doi:10.1021/acsenergylett.6b00247

Verger, L., Xu, C., Natu, V., Cheng, H.-M., Ren, W., and Barsoum, M. W. (2019). Overview of the Synthesis of MXenes and Other Ultrathin 2D Transition Metal Carbides and Nitrides. *Curr. Opin. Solid State. Mater. Sci.* 23, 149–163. doi:10.1016/j.cossms.2019.02.001

Wang, X., Kajiyama, S., Iinuma, H., Hosono, E., Oro, S., Moriguchi, I., et al. (2015). Pseudocapacitance of MXene Nanosheets for High-Power Sodium-Ion Hybrid Capacitors. *Nat. Commun.* 6, 6544. doi:10.1038/ncomms7544

Wang, Y., Xu, Y., Hu, M., Ling, H., and Zhu, X. (2020). MXenes: Focus on Optical and Electronic Properties and Corresponding Applications. *Nanophotonics* 9, 1601–1620. doi:10.1515/nanoph-2019-0556

Xuan, J., Wang, Z., Chen, Y., Liang, D., Cheng, L., Yang, X., et al. (2016). Organic-Base-Driven Intercalation and Delamination for the Production of Functionalized Titanium Carbide Nanosheets with Superior Photothermal Therapeutic Performance. *Angew. Chem. Int. Ed.* 55, 14569–14574. doi:10.1002/anie.201606643

Yang, S., Zhang, P., Wang, F., Ricciardulli, A. G., Lohe, M. R., Blom, P. W. M., et al. (2018). Fluoride-Free Synthesis of Two-Dimensional Titanium Carbide (MXene) Using A Binary Aqueous System. *Angew. Chem. Int. Ed.* 57, 15491–15495. doi:10.1002/anie.201809662

Yun, T., Kim, J.-S., Shim, J., Choi, D. S., Lee, K. E., Koo, S. H., et al. (2017). Ultrafast Interfacial Self-Assembly of 2D Transition Metal Dichalcogenides Monolayer Films and Their Vertical and In-Plane Heterostructures. *ACS Appl. Mater. Inter.* 9, 1021–1028. doi:10.1021/acsami.6b11365

Zhou, B., Li, Z., Li, Y., Liu, X., Ma, J., Feng, Y., et al. (2021). Flexible Hydrophobic 2D Ti3C2Tx-Based Transparent Conductive Film with Multifunctional Self-Cleaning, Electromagnetic Interference Shielding and Joule Heating Capacities. *Composites Sci. Tech.* 201, 108531. doi:10.1016/j.compscitech.2020.108531

Conflict of Interest: The authors declare that the research was conducted in the absence of any commercial or financial relationships that could be construed as a potential conflict of interest.

Publisher's Note: All claims expressed in this article are solely those of the authors and do not necessarily represent those of their affiliated organizations, or those of the publisher, the editors and the reviewers. Any product that may be evaluated in this article, or claim that may be made by its manufacturer, is not guaranteed or endorsed by the publisher.